The effect of aluminium on the electrical and mechanical properties of BaTiO₃ ceramics as a function of sintering temperature

Part 2 Mechanical properties

T. V. PARRY*, H. M. AL-ALLAK, G. J. RUSSELL, J. WOODS
*Applied Mechanics and Applied Physics Groups, School of Engineering and Applied Science, University of Durham, Science Laboratories, South Road, Durham DH1 3LE, UK

The effect of aluminium additions on the mechanical behaviour of BaTiO₃ positive temperature coefficient of resistance ceramics sintered in air at temperatures ranging between 1220 and 1400°C has been investigated. Tensile strength has been measured indirectly by the diametral compression of lapped discs using concave loading anvils. Values of ~ 85 and ~ 110 MPa for samples fired near their optimum sintering temperature were determined for two batches of material, the latter of which contained additions of Al_2O_3 (0.55 mol %). Strength did not vary systematically with grain size and appeared to be controlled by near surface defects. The size of these cavities, which were generally crescent shaped, was consistent with the material having a bulk fracture toughness of ~ 1.3 MPa m$^{1/2}$. The higher mechanical strength of samples which contained Al_2O_3 additions was attributed to the enhanced "healing up" of these cavities by the liquid phase giving a smaller inherent critical defect size rather than by increasing the bulk toughness of the ceramic.

1. Introduction

In Part 1 [1], the effect of aluminium additions, introduced in the form of Al_2O_3, on the electrical behaviour of barium titanate positive temperature coefficient of resistance (PTCR) ceramics was presented as a function of sintering temperature. As well as the importance of their electrical properties, the mechanical performance of these materials is now of increasing significance. In particular, devices subjected to mains voltages, ~ 240 V$_{a.c.}$, must be capable of withstanding stresses which derive from thermal shock when the device is switched on and off. Repeated switching of the device can cause cracks to develop within the material which grow with continued thermal cycling. The propagation of these cracks through the component causes a detrimental increase in the resistance of the device. There is therefore an interest in the strength and toughness of barium titanate for PTC device applications.

Tension testing of brittle materials directly, though desirable, is notoriously unreliable due to the difficulties associated with specimen preparation and alignment during testing. Measurement of tensile strength in bending using three- or four-point loading has therefore been widely adopted. The maximum tensile stress on the convex surface of the beam is calculated from the load at failure from simple bending theory and is frequently called the "modulus of rupture". This value is approximately equal to the tensile strength if allowance is made for any differences in volume of material subjected to the maximum stress [2].

An indirect method of determining the tensile strength of brittle materials is the diametral compression test or Brazilian test [3]. In its simplest form, the test involves the compression of a disc-like specimen along the vertical diameter, where failure eventually takes place. The correlation between values measured by this and other tests on the same material varies from good, for some rocks [4], to poor for materials such as polycrystalline alumina and magnesia [5]. Invariably the diametral compression test underestimates the tensile strength of the material by up to 50% in certain cases [6]. This has been attributed to the biaxial state of stress experienced by the sample [7]. The induced tensile stress on the vertical plane is accompanied by an orthogonal compressive stress of three times its magnitude.

It has also been recognized that stress concentrations at the loading lines can lead to premature failure initiation in these regions. For example, it has been suggested that the use of brass shims at the loading contacts can reduce these problems [8]. An alternative approach has been reported to suppress specimen collapse at the contact edges by superimposing a Hertzian contact stress distribution on the test system [9]. This was achieved by the use of concave, as opposed to plane, loading anvils. It was shown that when the ratio of the contact half width to the radius of the specimen (b/R) was small, the value of strength measured varied linearly with this ratio. However, when it exceeded ~ 0.27, strength values were independent of this parameter. This phenomenon was
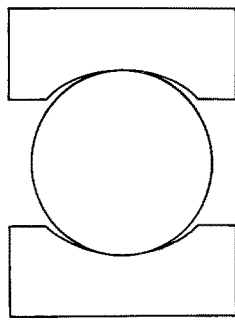
Figure 1 Diametral compression test geometry showing concave loading anvils.

Figure 3 Polished section of a failed sample showing typical mode of failure. Note the single fracture on the diametral plane and absence of significant damage at the loading contact.

interpreted in terms of the shear stress distribution within the sample. For small values of b/R, a high shear stress near the loading contact was observed. Failure at lower loads could therefore be initiated prematurely due to highly localized shear stresses in these regions rather than at the centre of the specimen where the tensile stress is highest [10]. It was suggested that the latter mode of failure is more likely if the ratio of radius of curvature of the loading anvils to the radius of the test specimen is ~ 1.25.

As barium titanate PTCR ceramics are currently sintered in the form of discs both for device applications as well as electrical property measurements [1], this particular mechanical test method appears to be most appropriate to assess the effect of processing variables on the strength of these materials.

Aluminium has been advocated widely as a sintering aid which improves the electrical properties of the final device [11]. It has also been shown in the first part of this communication that such additions increase the volume of the liquid phase. The object of this paper is to report the effects of additions of Al_2O_3 on the mechanical properties of the fired ceramics.

2. Experimental methods

All samples tested in this investigation were taken from the same batches prepared for the electrical characterization reported previously [1]. The as-sintered compacts were in the form of discs ~ 4.5 mm diameter and ~ 2.5 mm thick. These dimensions were selected because they correspond to those of manufac-

tured PTC devices. Non-uniform and temperature-dependent shrinkage during the liquid-phase sintering process had the effect of producing a concave circumferential edge to the pellets. To regain a uniform circumference, which was to be loaded, the specimens were lapped on a Logitech precision polishing machine. The machine was fitted with a purpose-built attachment which maintained a cylindrical profile to the pellets. This permitted them to rotate within slots in a locating plate due to the counter rotation of an upper lapping surface. The whole device oscillated slowly on the standard plate of the machine which maintained a differential speed with respect to the upper surface which produced the lapping action. The lapping medium was 0.1 μm diamond paste. Uniform profiles on up to 12 samples were produced typically within 15 to 30 min.

Mechanical testing was carried out on an Instron 1000 bench testing machine with a 5 kN capacity. Load and cross-head displacement were monitored autographically using a loading rate of ~ 3.5 mm min^{-1}. Failure was detected by an audible crack accompanied by a drop in load on the autographic trace. In the cracked condition the sample retained significant load-carrying capacity and care had to be taken to ensure that it was unloaded immediately to avoid secondary failures. The loading anvils employed had a radius of curvature of 2.75 mm and are shown schematically in Fig. 1.
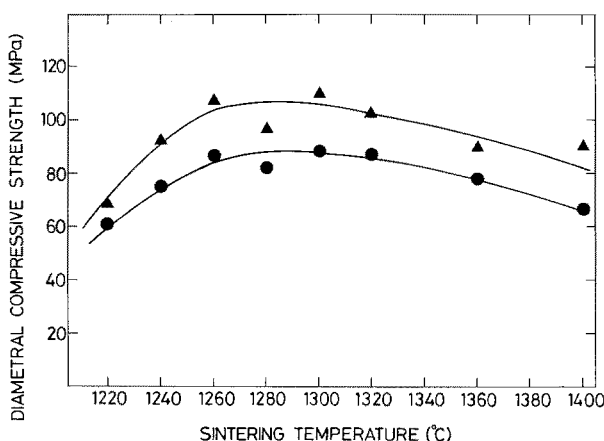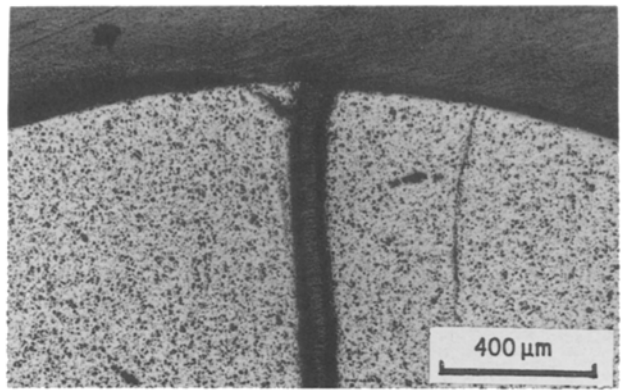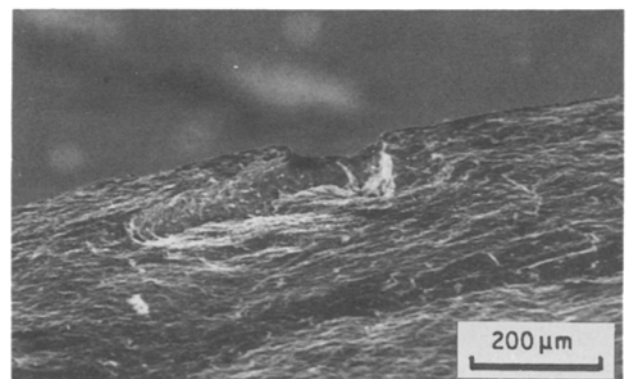

Figure 2 Dependence of diametral compressive strength on sintering temperature for samples (▲) with and (●) without alumina additions.

Figure 4 Scanning electron fractograph of a sample to which alumina additions had not been made. Note the failure origin $\sim 500 \mu$m $\times$ $\sim 170 \mu$m located at the specimen surface.

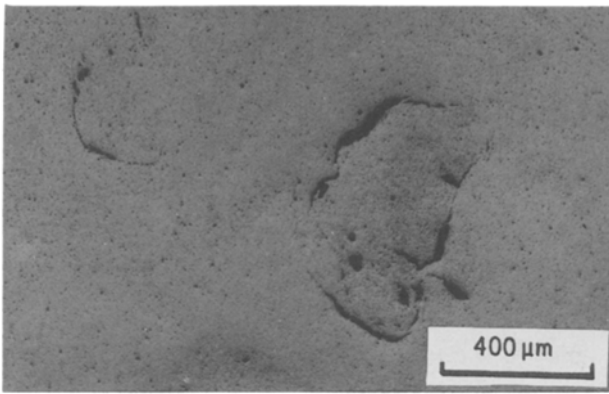*Figure 5* Polished, unetched, section of a sample containing alumina additions sintered at 1240°C. Note the crescent-shaped defects.

Figure 7 Polished, unetched, section of a sample containing alumina additions sintered at 1320°C. Note how by this temperature the defects have become smaller and more regular.

Fracture-surface examination and grain-size determinations were carried out using Cambridge Instruments S600 and S180 scanning electron microscopes. Optical examination of polished as-sintered samples was achieved using a Zeiss Ultraphot II microscope.

3. Results

The mean grain size of the sintered ceramics with (type A) and without (type B) alumina additions are shown in Table I as a function of sintering temperature.

Values of diametral compressive strength, σ, were calculated from the peak load at failure using the following relation [10]

$$\sigma = \frac{2P}{\pi dt} \tag{1}$$

where P is the maximum compressive force on a sample of diameter, d, and thickness, t. The variation of this parameter with sintering temperature is plotted for type A and type B materials in Fig. 2. Failure was by a single crack on or near the diametral plane as shown in Fig. 3. For some samples, the material in the vicinity of the loading regions was uncracked and the two halves of the failed specimen had to be separated subsequently to reveal the fracture surfaces. Failure origins were readily located by scanning electron fractography for the type B material. A typical example is presented in Fig. 4. Failure origins were less readily identified, however, for the samples to which the additions had been made. Therefore, polished,
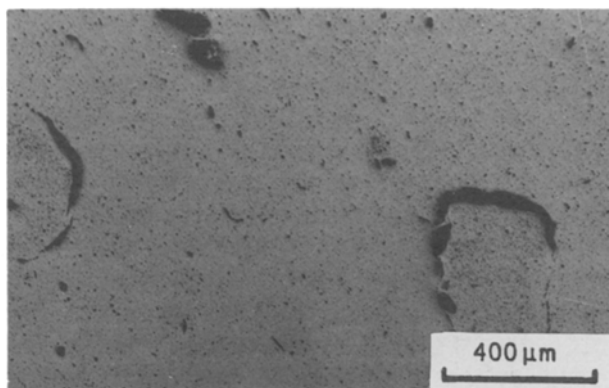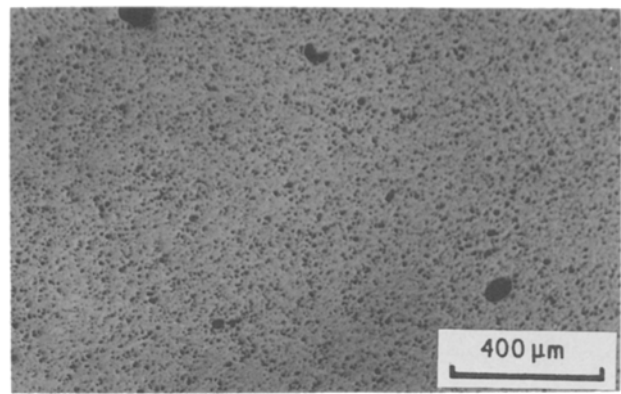

Figure 6 Polished, unetched, section of a sample without alumina additions sintered at 1240°C. Note the similarity in defect shape to Fig. 5.

unetched, sections were examined under the optical microscope to reveal the size and distribution of defects in unstressed samples. In undersintered samples these generally appeared crescent shaped in two-dimensional section. Figs 5 and 6 are of optical micrographs of samples with and without alumina, respectively, sintered at 1240°C. At higher sintering temperatures the cavities in the former material tended to become smaller and more regular (Fig. 7) whereas for the latter, Fig. 8 shows that crescent-shape defects persisted. Fig. 9 is a composite section of a fractured type B sample which had been sintered at 1400°C and shows a defect of this type, part of which appears to have acted as a failure origin.

4. Discussion

The mode of failure shown in Fig. 3 is typical of those observed in this investigation and demonstrates that premature failure initiation at the loading contacts, often associated with this test, appears to have been inhibited. The fact that for some samples crack arrest took place within the compressive stress field associated with these contacts is a further indication that failure originated away from these regions. The values of tensile strength measured indirectly by this test for samples fired at or near their optimum sintering temperature, vary between ~ 85 and $\sim 110\,\mathrm{MPa}$. This is in general agreement with data reported recently by DeWith and Parren [12] for a series of commercially available PTC ceramics doped with various proprietary additives. They found that values of strength measured using miniature three-point bend specimens

TABLE I The effect of sintering temperature on the mean grain size of ceramics containing alumina additions (type A) and those such additions (type B)

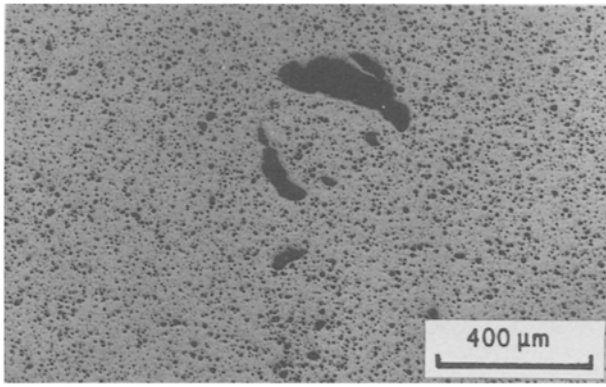| Sintering temperature (°C)	Mean grain size (μm)	
	Type A material	Type B material
1240	1.8	2.0
1260	4.8	3.0
1280	5.3	3.8
1300	5.6	4.3
1320	6.0	4.3
1360	6.8	4.5
1400	5.7	5.2

Figure 8 Polished, unetched, section of a sample without alumina additions sintered at 1320° C. Note that the defect size and shape in Fig. 6, persist to this sintering temperature.
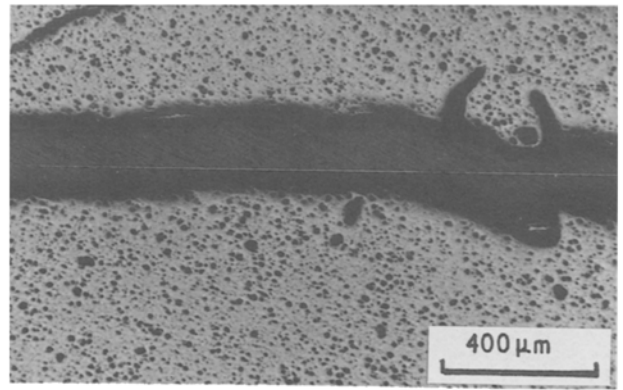

Figure 9 Polished, unetched, section of a fractured sample which had been sintered at 1400° C. Note that in the absence of alumina additions crescent-shaped defects persist to the highest sintering temperature employed and, in this particular example, appears to have acted as a failure origin.

ranged from ~ 100 to ~ 140 MPa. Bend testing and small specimens tend to overestimate tensile strength and if the volume of material subjected to the maximum stress for each test is taken into account [2], the difference between the values is therefore probably not significant. The test used in this investigation, however, is capable of detecting bulk as well as surface defects.

Inspection of Fig. 2 and Table I reveals that the strength of both type A and type B materials does not vary systematically with grain size. In particular, the inverse dependence of the fracture stress on the square root of the mean grain size, reported for other ceramics [13], was not observed. This, together with Figs 5 to 9, would suggest that the strength of this material is controlled by inherent defects which are significantly larger than the average grain size. However, the defect-controlled strength of brittle materials can only be fully characterized if the fracture toughness is known. A value of $K_{IC} = 1.3$ MPa m$^{1/2}$ has been reported recently for a range of similar PTC ceramics [12]. If it is assumed that a similar value is applicable here then the critical defect size, a_{crit}, can be calculated from [12]

$$K_{IC} = \psi \sigma_f (a_{crit})^{1/2} \qquad (2)$$

where ψ is a dimensionless geometrical factor and σ_f is the fracture stress. The precise value of ψ will depend upon the configuration and location of the defect within the sample. If this parameter is assumed to be unity, a reasonable estimate of the critical defect size can be obtained. Taking values of fracture stress from Fig. 2 and a value of $K_{IC} = 1.3$ MPa m$^{1/2}$ [12], these range from 140 to 380 μm and 210 to 440 μm for type A and type B material, respectively. The feature shown in Fig. 4 is $\sim 500 \mu$m $\times$ 170 μm and was observed in a sample of type B material with a fracture strength of 68 MPa from which the theoretical defect size evaluates to $\sim 360 \mu$m. This is in good general agreement despite the simplifying assumptions made.

The source of failure shown in Fig. 4 is typical of those observed for type B material. No significant differences in local composition were detected by EDX spectra and Figs 5 and 6 suggest that they originate as crescent-shaped cavities which do not close during early sintering or in the absence of alumina

additions. The appearance of the inner surfaces has the same general characteristics of the "as-sintered" surfaces described previously [1] and even include similar fibrous features. It is likely that these cavities can be traced back to the pressing stage of the preparation process as their shape is largely unaltered by sintering temperature for type B material. They appear to be located and oriented randomly throughout the bulk of the material and failure ensues from the largest and least favourably oriented portion of the defect with respect to the maximum stress, as suggested by Fig. 9.

The role of alumina in promoting the liquid phase appears to have had two effects on these pressing defects, the first of which is to reduce their size. Secondly, the shape of the defects becomes more regular with an aspect ratio approaching unity. Both of these trends will produce a ceramic with higher strength and are consistent with the observation that, for the same sintering conditions, type A material was always stronger than type B material. Fracture behaviour, however, for both materials was similar and invariably transgranular (Fig. 4).

In conclusion, it has been demonstrated that the diametral compression of carefully lapped discs using concave loading anvils can provide an indirect measurement of the tensile strength of BaTiO$_3$ PTC ceramics. This strength has been shown to be controlled by the presence of crescent shaped defects which probably originate from the pressing stage and persist for all sintering temperatures investigated for material which does not contain additions of alumina. The increased strength shown by samples to which these additions had been made can be attributed to a smaller (inherent) critical defect size — as the defects partly "heal up" during sintering — as opposed to any increase in toughness of the bulk ceramic.

Acknowledgements

Materials, University of Bradford, for the provision of optical microscope facilities.

Whilst this paper was being considered, Dr Graham J. Russell was tragically killed in an accident. His enthusiastic contribution to this and other research work will be sadly missed.

References
1. H. M. AL-ALLAK, T. V. PARRY, G. J. RUSSELL and J. WOODS, *J. Mater. Sci* **23** (1988) 1083.
2. A. G. EVANS, in "Fracture Mechanics of Ceramics", Vol. 3, edited by R. C. Bradt, D. P. H. Hasselman and F. F. Lange (Plenum, New York, 1978) p. 31.
3. F. L. L. B. CARNIERO and A. BARCELLOS, Union of Testing and Research Laboratories for Materials and Structures, no. 13 (1953).
4. M. MELLOR and I. HAWKES, *Engng Geol.* **5** (1971) 173.
5. M. S. STUCKE and A. S. WRONSKI, *Proc. Brit. Ceram. Soc.* **25** (1975) 109.
6. R. M. SPRIGGS, L. A. BRISSETTE and T. VASILOS, *Mater. Res. Stand.* **4** (1964) 218.
7. O. VARDAR and I. FINNIE, *Int. J. Fracture* **11** (1975) 495.
8. M. C. SHAW, P. M. BRAIDEN and G. J. DeSALVO, *Trans ASME, J. Engng Ind.* **97** (1975) 77.
9. H. AWAJI and S. SATO, *Trans ASME, J. Engng Mater. Technol.* **101** (1979) 139.
10. H. AWAJI, *ibid.* **102** (1980) 257.
11. J. W. FLEMING, H. M. O'BRYAN and J. THOMSON, US Pat. 4 175 060 (1979).
12. G. DE WITH and H. PARREN, in "Science of Ceramics", Proceedings of the 12th International Conference, Saint-Vincent, Italy (1984) p. 537.
13. R. C. POHANKA, S W. FREIMAN and B. A. BENDER, *J. Amer. Ceram. Soc.* **61** (1978) 72.